Challenging Glass 5 – Conference on Architectural and Structural Applications of Glass
Belis, Bos & Louter (Eds.), Ghent University, June 2016.

ISBN 978-90-825-2680-6

Experimental and Numerical Study on Glass Stresses and Shear Deformation of Long Adhesive Joints in Timber-Glass Composites

F. Nicklisch, J. Giese-Hinz & B. Weller
Technische Universität Dresden, Germany, felix.nicklisch@tu-dresden.de

This study assesses the shear strength of long adhesive joints on mid-size specimens to resemble virtually a life-size situation in a typical timber-glass composite element. The specimens comprise a rectangular glass pane which is adhesively bonded along its vertical edges onto timber posts. The study focuses on three different adhesives ranging from flexible silicones to viscoplastic epoxies with a high stiffness. In the experiment, the adhesive joints are stressed in longitudinal shear and loaded until failure.The experiment is simulated using a numerical model of the specimen. The joint is described by basic material models taking into account linear or bilinear behavior of the adhesive material. The corresponding material properties of the adhesives were derived from uniaxial tensile tests on the cured adhesive. The stiff adhesive causes high stress concentrations close to the edge where the load is applied. More flexible joints lead to a more homogenous distribution since the shear loading result in higher compressive stresses in the lower parts of the glass pane. Finally, we compare the results from the experiment and the numerical simulation by means of glass stresses and shear deformation of the adhesive bond line. It can be shown that bilinear constitutive equations are an adequate approximation of the adhesive to determine the glass stresses in the pane. However, the deformations could not be reproduced for all adhesives in the same accuracy than the stresses.

Keywords: Structural glass, timber-glass composites, adhesive bonding, FEA, numerical simulation

1. Introduction

Wooden constructions are on the rise again – encouraged by a strong public and economic trend towards sustainable and resource efficient buildings. Spurred by this growing interest novel design principles and material assemblies in architecture and the building industry evolve. These developments require further research due to the absence of evaluation tools and insufficient knowledge about their design.

Load-bearing timber-glass composite elements could contribute to a more efficient use of materials in façade constructions. Fig. 1 shows a general build-up of such a shear wall element. In this case a linear adhesive bond connects the glass pane to the timber substructure. This enables an in-plane loading of the glass whose capacity is not used to its full potential in conventional façades as it is solely applied as an infill panel. First concepts for a timber-glass composite structural element for shear walls were developed by Hamm (2001). Initially, the glazing was glued directly on the timber frame construction. The wooden adapter frame is proposed by Niedermaier (2005). It improves the system as it enables prefabrication of the composite element in the shop as well as an easy removal and exchange of damaged glass panes. This adapter is further enhanced by means of a serrated shape. Shifted frames of adjacent elements fit together which lead to slender faces of transom and mullions (Edl 2008).

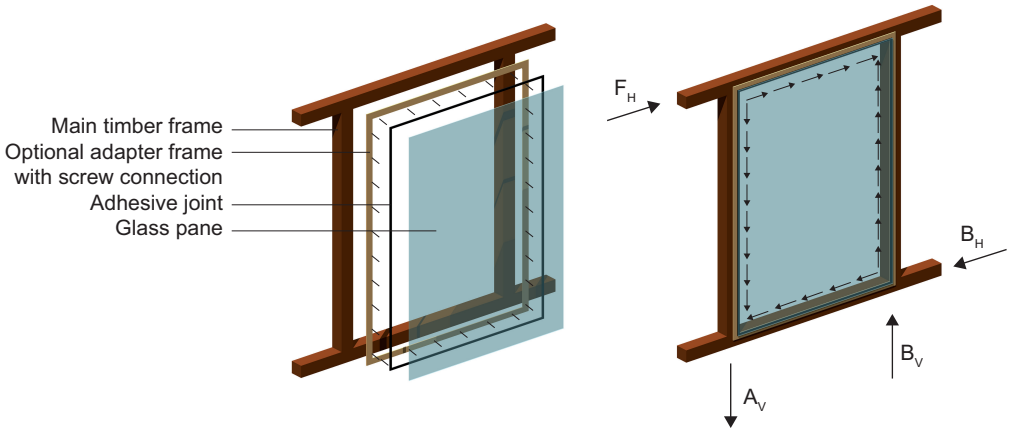

Fig. 1 General build-up and load-bearing principle of a timber-glass shear wall element according to Edl (2008)

Such timber-glass composite elements comprise long adhesive joints since the glass pane is bonded circumferentially. In general, those bond lines are exposed to longitudinal shear. Hochhauser et al. (2013) developed calculation methods for such load-bearing timber glass shear walls based on spring models. The approaches apply to a circumferential bond or to a combination of an elastic joint and a stiffer blocking system.

The assumption of uniformly distributed stress along the linear joint is not accurate, especially when stiffer adhesives are used. Peak stresses occur at both ends of the joint. Hence, ultimate strength of the adhesive may be reached at those points while the remaining part of the bond is not fully loaded. Therefore, this study assesses the shear strength of long adhesive joints on mid-size specimens to resemble virtually a life-size situation in typical timber-glass composite elements.

Structural sealants such as silicones, which are commonly used for the joint, provide a high flexibility and only a low load-bearing capacity. Considering such elements being part of a bracing system, the mentioned characteristics limit the application range to buildings with not more than two floors. Hence, this scope can be widened by high-modulus adhesives, which have not yet been evaluated for their use in building constructions. Three different adhesives exhibiting very different stiffness and strength are tested in total. The general stress distribution in the glass pane is assessed using strain gauges and photoelastic analysis. The experimental results are verified by numerical simulation using a linear or bilinear approach.

2. Materials

2.1. Adhesives

Three adhesives are used for the experimental evaluation of the bond strength and for the material models in the numerical simulation. The selection bases on thorough material characterization of a broad spectrum of potential adhesives in Weller et al. (2013) and Nicklisch et al. (2014). An intermediate- and a high-modulus adhesive qualified as suitable for timber-glass composite construction. The silicone adhesive complements the test series to serve as a reference material to the current practice. Table 1 summarizes the properties of the adhesives derived by mechanical testing of the bulk material. The test procedure followed the guidelines according to EN ISO 527-1:2012-06.

Table 1 Adhesives and basic material constants (Weller et al. 2013)

ID	Adhesive	Manufacturer	Type/chemical basis	E [N/mm^2]	μ	ε_{max} [-]
A	OTTOCOLL® S660	Hermann Otto GmbH	Two-part silicone	3	0.50	1.65
B	nolax C44.8505	nolax AG	Two-part silane modified epoxy	18	0.39	1.99
C	Scotch-Weld™ DP490	3M	Two-part epoxy	1,442	0.43	0.05

2.2. Timber and glass components

The mid-size shear specimens comprise a timber and a glass part. The choice of glass depends on the expected ultimate loads. All silicone bonded specimens are made of annealed float glass of 8 mm nominal thickness. Tempered soda-lime glass of 8 mm nominal thickness is used with the remaining adhesives. Its higher strength compared to that of standard float glass minimizes the risk of glass failure during testing at higher loads. In any case, the tempering of the glass does not change adhesion characteristics of the surface. All glass edges are polished. It was decided to glue only onto the air-side of the glass, which is determined by means of UV-inspection.

Glass exhibits an ideal elastic material behavior without any plastic deformability. The German standard about glass in Building DIN 18008-1:2010-12 provides fundamental material characteristics. The numerical calculations presented in this paper involve a Young's Modulus of E_{glass} = 70,000 N/mm^2 and a Poisson's Ratio of μ = 0,23.

Birch plywood, a wood-based material made from cross-laminated birch veneers, was used in the tests. It relates to the state-of-the-art in timber-glass composite construction, since the adapter frame of a commercially available timber-glass composite façade system (uniGlas® GmbH 2014) is manufactured from this material. Plywood shows excellent shape stability and reduced tendency of shrinkage. It was glued such that the veneers were parallel to the bond line plane and the fiber direction of the outer layer was parallel to the loading direction. The material properties were taken from the producer's technical sheet (Finnforest 2001). An 18 mm thick birch plywood panel offers an average Young's Modulus under tensile loads of $E_{t,||}$ = 9,150 N/mm^2.

3. Experimental evaluation of long adhesive joints

Testing on a larger scale provides extra benefits as the long linear adhesive joints resemble virtually the situation in a real-size element. The mid-size specimen (Fig. 2 and Fig. 3) used in this test series comprises a glass pane measuring 500 x 1000 mm. The glass is glued along its vertical edges to an adapter frame made of birch plywood. The load – applied in vertical direction – stresses the joint in longitudinal shear. The size of the plywood adapter and

the glass type was chosen according to the structural requirements. Based on the failure loads taken from small specimen tests, higher load-bearing capacity is expected for the selected adhesives with intermediate (B) and high stiffness (C). Hence, the specimens bonded with the silicone adhesive (A) comprising an annealed float glass pane and a 12 mm thin birch plywood adapter. The specimens designed for high loading were made from fully toughened glass and an adapter with a larger cross-section. The joint geometry stays the same for all specimens.

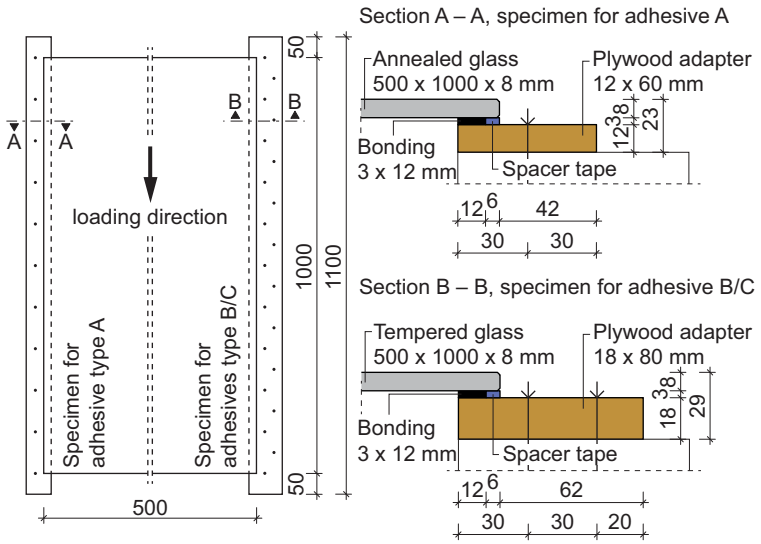

Fig. 2 Specimen configuration for mid-size shear tests

Fig. 3 Prepared specimen with two long joints made from adhesive C – DP490

The specimen is fastened to a specific test rig shown in Fig. 4. The upper cross-head holds a hydraulic jack, the piston is facing downwards. The load is applied to the center axis of the glass pane via a plate which is guided in vertical direction by two linear shafts. A steel traverse which can rotate freely is attached to the bottom side of this plate. This traverse allows for an equal load distribution to the two plastic setting blocks sitting on the upper edge of the glass pane. The load application device is released after the specimen is aligned and fastened onto the test rig. The hydraulic jack is loaded by a manual pump. The force is raised continuously until the specimen fails. The force is recorded by a load cell. Two displacement transducers – one on the left and one on the right side – measure the relative displacement between the birch plywood adapter and the glass edge.

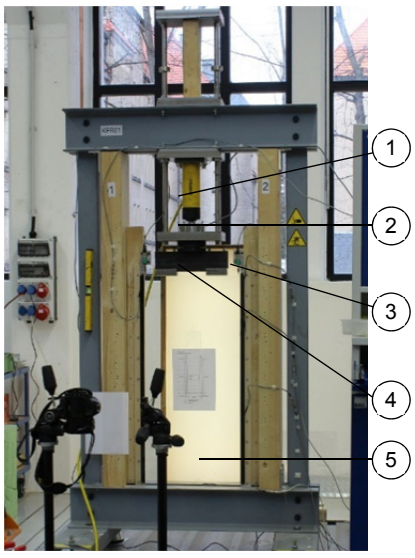

Fig. 4 Timber-glass specimen (5) mounted on the test rig with hydraulik jack (1), load cell (2), displacement transducer (3), load transfer to glass edge (4)

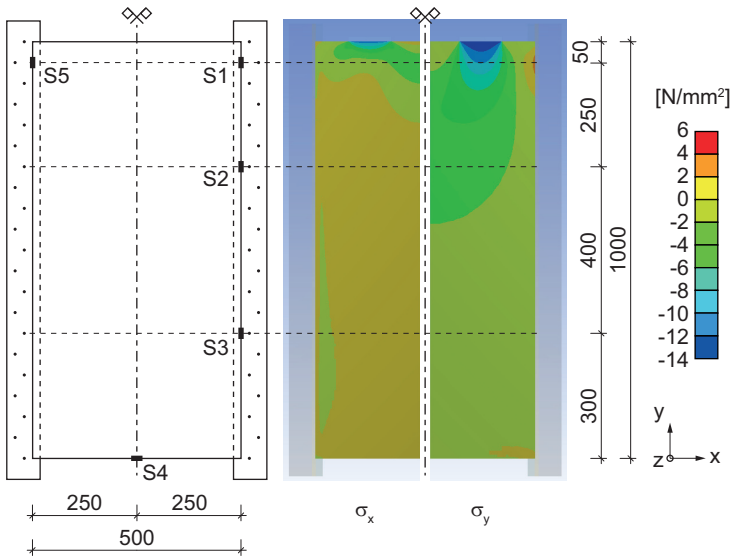

Fig. 5 Strain gauge positions (DMS) and stresses derived from a finite element analysis using a linear elastic material model for the joint (adhesive C – DP490, loading 20 kN)

The load bearing capacity of the adhesive bond with a length of 1000 mm is determined on a minimum of five specimens per adhesive. Strain gauges enable the evaluation of strain and stresses in the glass. Fig. 5 shows their positions which are defined on the basis of the computed stress distribution in the glass pane. Three sensors (S1 to S3) are attached to the vertical glass edge. Another strain gauge (S4) is located in the center of the bottom edge. Position S1 and S5 serve as reference values to monitor an equal load transfer to both bond lines.

Photographic images of the backlit glass using a polarizing filter enable an initial assessment of the general stress distribution in the glass. The light source with the polarizer is located behind the glass pane. The camera equipped with the filter (analyzer) is placed in front of the rig. Strain measurements and photoelastic analysis are conducted only on a few specimen.

4. Numerical model

The experiments were simulated numerically by finite element method using ANSYS Workbench R15.0. The generated model (Fig. 6) of the mid-size specimen comprises the glass pane, the adhesive joint and the adapter frame as well as the blocking where the load is applied. The latter provides a homogenous load transfer and eliminates singular stress peaks. Only one half of the specimen is modelled by taking the symmetry of loading and boundary conditions into account.

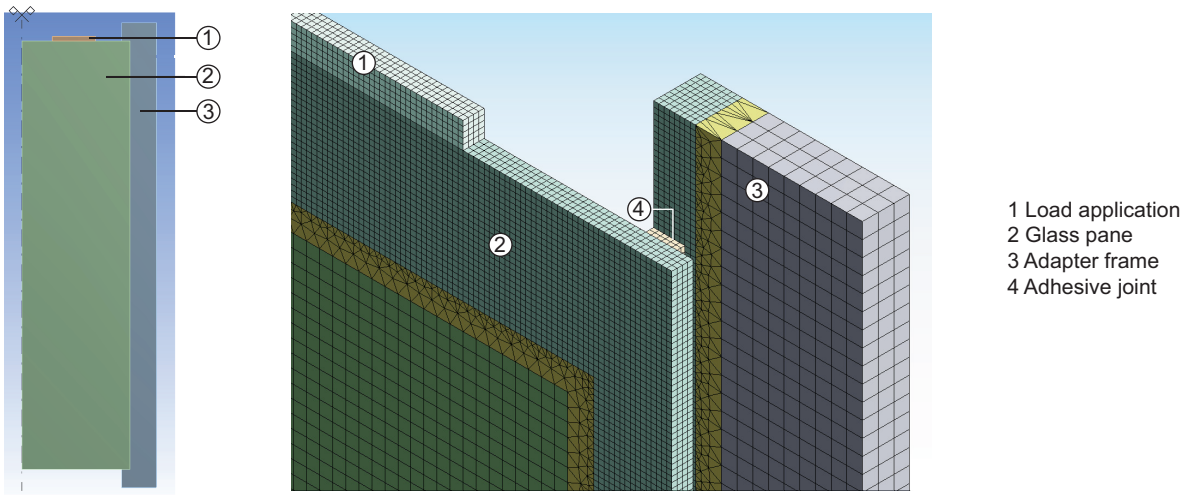

Fig. 6 Geometry and meshing of the numerical model

All components of the three-dimensional geometry are idealized with homogenous structural solids. The higher order 20-node elements (SOLID186) supports numerous constitutive models. Eight nodes at the corners define the hexahedral solid. Each edge further comprises an intermediate node which improves the accuracy of the computation. In this case, we approximate all materials with isotropic properties. In this basic numerical calculation the deformation behavior of the adhesive is idealized by linear elastic or bilinear elastic material models.

The generated mesh is coarse in the center and fine along the boundary of the glass pane, where loads are applied or transferred via the bond. The edge length of the small finite elements is fixed to 2 mm. The fine meshing applies also to the adhesive joint and the adapter frame within close distance to the bonded surface. In this sector the outer nodes of the joint match with the nodes on the surface of the glass or the wooden adapter frame, respectively. The load is uniformly distributed on all nodes of the upper surface of the blocking. The degrees of freedom along the central axis comply with requirements of symmetry. The nodes on the rear side of the adapter frame are fixed to restrain movement in any direction.

Uniaxial tensile tests on standard specimens (Type 1A according to DIN EN ISO 527-2:2012-06) provide the stress-strain data to calibrate the material models. Those specimens are made from the pure adhesive material. The experiments are conducted at a loading rate of 1 mm/min. Testing ends at a maximum elongation of 50 % axial strain if the specimen has not failed until that point. A video extensometer is used to ensure noncontact measurement of the deformation of the specimen in axial and transversal direction. This test data was already published in extracts in Weller et al. (2013) and Nicklisch et al. (2014).

The nonlinear material behavior of the adhesives is approximated by linearization of the stress-strain curve using two straight lines. The material constant of the first section is calculated from the results between 0.05% and 0.25% axial strain. The slope of a regression line through all data points in this strain range equals the modulus value.

This stiffness corresponds to the modulus of elasticity also used in the linear elastic approach. In the second section, a tangent is drawn to a linear segment of the curve. The stress-strain data relates to the real area of the cross section which is determined from the continuously recorded transverse strain. The area decreases with the growing elongation in the tension test.

The stress-strain relationships at room temperature (Fig. 7) show the variances in material behavior of the adhesives examined. The difference between the silicone and the two other adhesives becomes clearly visible. The initial stiffness of nolax C44.8505 and Scotch-Weld DP490 is significantly higher than that of Ottocoll S660. The intersection of the bilinear approximation – between the initial modulus and the tangent modulus – varies depending on the specific material behavior.

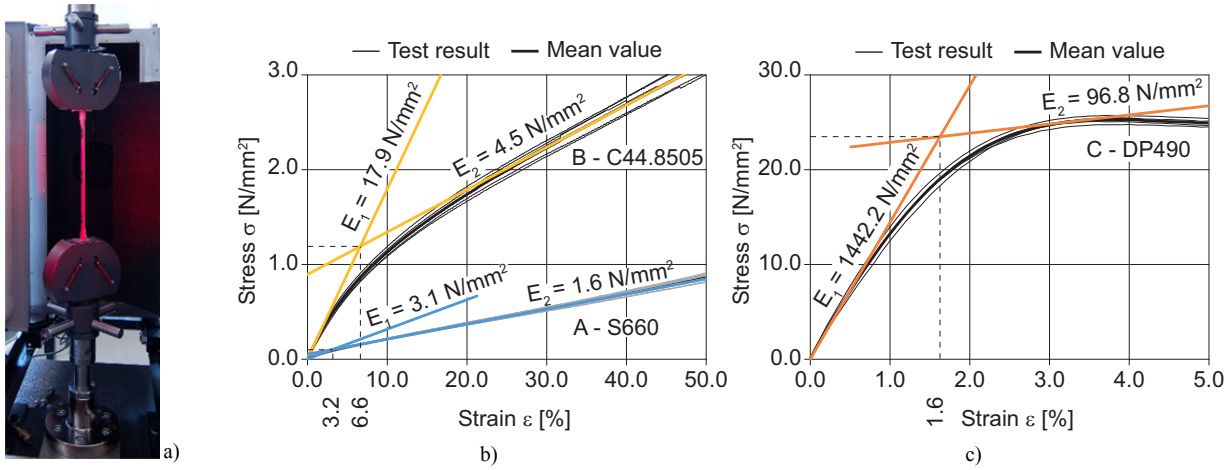

a) b) c)

Fig. 7 Tensile tests at room temperatur: a) Specimen under tensile load b) stress-strain data for A-Ottocoll S660 and B-nolax C44.8505, c) stress-strain data for C-Scotch-Weld DP490

The initial stiffness of Ottocoll S660 applies only to a short range up to around 2.0 % axial strain. After that point the curve progresses with a reduced gradient in an almost linear manner. In principle, the curve shape of nolax C44.8505 is similar to that of Ottocoll S660. But, its magnitude is more than five times higher and the initial stiffness persists over a wider strain range. Both adhesives exhibit a high flexibility and does not fail within the examined strain range. In contrast, the stiff epoxy adhesive Scotch-Weld DP490 shows a distinctive maximum load and a ductile behavior before failure. The epoxy specimens break at relatively low strain values ranging from approximately 4 to 8 %. Test results are only displayed up to 5 % axial stain. Close to the ultimate load the stress-strain relationship does not reveal a distinct linear section. Hence, the tangent is drawn to the curve within an assumed range between 3.0 % and 3.5 % axial strain.

5. Results and discussion

5.1. Stress distribution in the glass pane

The general stress distribution in the glass pane is evaluated by means of principal stresses resulting from a load of 20 kN. The computed results from a basic bilinear elastic model are shown for the right half of the glass surface viewed from the front. Tensile stresses (Fig. 8) concentrate in two zones. One maximum develops close to the upper part of the bond. The second tension zone is in the center of the bottom edge. Comparing the three adhesives, we detect a redistribution of the stress peaks relating to the stiffness of the adhesives. A distinct peak evolves with a higher stiffness of the adhesive joint in the upper part of the vertical edge, while the tensile stresses diminish in the bending zone at the horizontal edge. It is therefore indicated, that joints modelled with a higher stiffness transfer the major load over a shorter bond length into the adapter frame.

The main feature of the contour plot of the secondary principal stresses (Fig. 9) is the pressure bulb located right below the upper edge where the load is applied. The stress distribution is almost similar for the three adhesives at this point. That changes slightly in the lower part of the glass. The shapes of the contours illustrate that a flexible joint lead to a more homogenous load transfer over the adhesive bond. Hence, glass stresses along the vertical edge where the glass is glued onto the plywood adapter are distributed more evenly. With the stiff epoxy adhesive the lower part of the glass pane keeps rather unstressed.

A photoelastic study of the glass corroborate those findings. Stress-free areas or regions where the difference of the principal stresses equals zero appear black. Bright or colored zones highlight areas where this difference is relatively large. The boundary between dark and light regions is outlined with a colored line in the images taken with a polarizing filter (Fig. 10). The pattern in the glass specimen, which are glued with the adhesives nolax C44.8505 or Scotch-Weld DP490, has its cause in the type of glass. The light which passes through the thermally treated glass experiences double refraction. An inhomogeneous residual stress state causes this pattern. It originates from the cooling process.

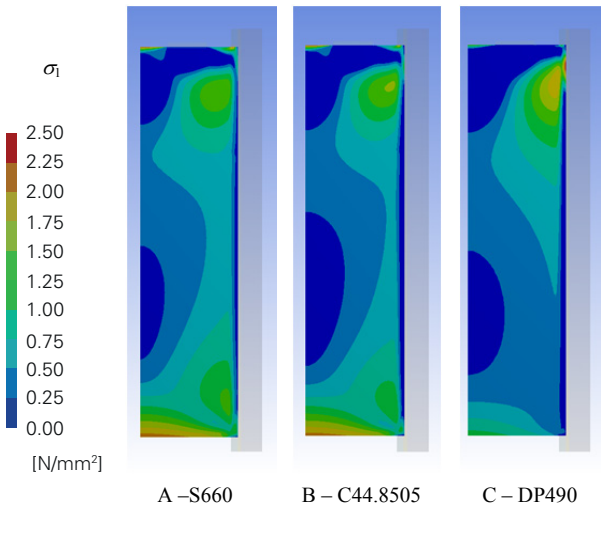

Fig. 8 Priniciple stress σ_1 (tension) in the glass pane (right half), specimen loaded by 20 kN

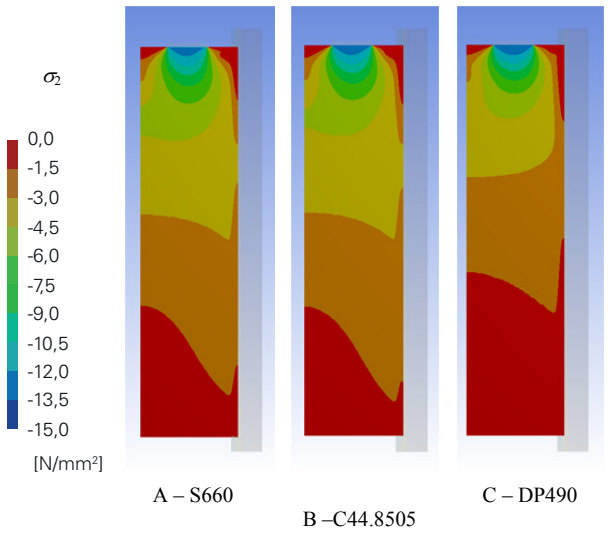

Fig. 9 Priniciple stress σ_2 (compression) in the glass pane (right half), specimen loaded by 20 kN

The boundaries drawn in Fig. 10 are almost congruent below the load application point. However, the marking differs in the range of the vertical glass edge. The bright area diminishes for the adhesives exhibiting a higher rigidity. The image taken from the specimen glued with a flexible silicone reveals instead a uniform distribution over the entire length of the vertical glass edge. This indicates a homogeneous load transfer over the adhesive joint.

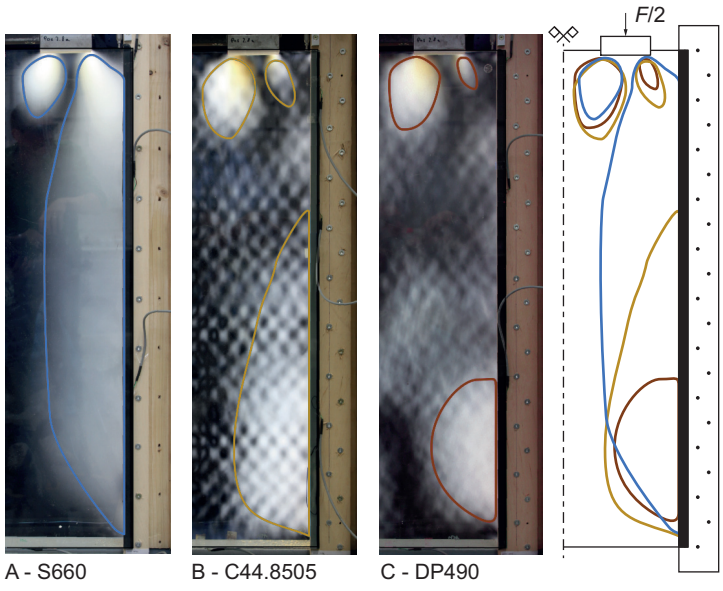

Fig. 10 Images of the backlit glass pane (right half) taken with a polarizing filter, specimen loaded by 20 kN

5.2. Deformation and strength of the long joint

The load-displacement relation of three different specimens is shown in Fig. 11. The results derived from the experiment are compared to the computed deformation in the numerical simulation. Calculation and experiment coincide roughly for the flexible silicone and for the stiff epoxy. The calculated deformation of nolax C44.8505 runs far from the values measured by the displacement transducers.

The silicone specimen (A – Ottocoll S660) fails at slightly above 20 kN by internal rupture of the adhesive joint. This cohesive failure is shown in Fig. 12. The short-term testing of the other two adhesives (B – nolax C44.8505 and C – Scotch-Weld DP490) reveals a significant increase of load-bearing capacity compared to that of silicones. The high-strength joints fail mainly by rupture of timber fibers on the surface (Fig. 12). At the same time the shear deformation could be reduced considerably. The average vertical displacement of the joints produced with nolax C44.8505 (B) is just slightly below 1 mm in the moment of failure. Displacement readings from the tests on components glued with Scotch-Weld DP490 (C) are rather difficult to interpret. The high stiffness of the adhesive leads to nearly "zero" displacement in the experiment. The force-displacement relation is overlain by other effects such as signal noise or minor negative values related to the deflection of the whole test rig.

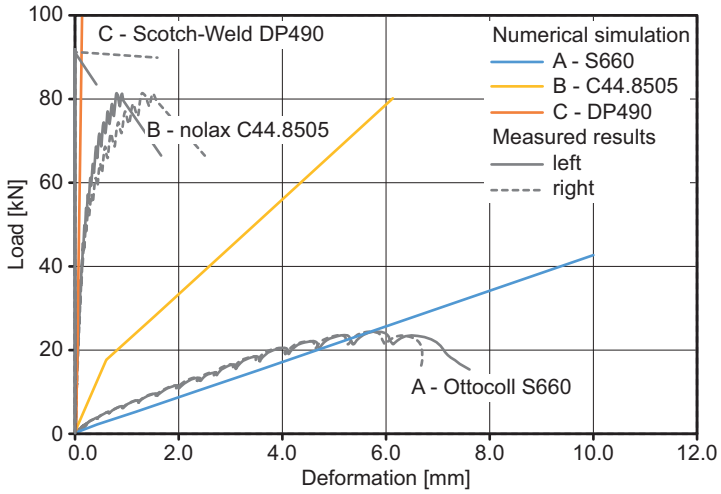

Fig. 11: Representative load-displacement relation from mid-size shear tests on three different adhesives

Fig. 12: Failure modes

The ultimate shear strengths of components with nolax C44.8505 and with Scotch-Weld DP490 differ marginally, although the related stiffness values of the bulk material diverge more widely. It is assumed that a threshold value is reached which is not significantly influenced by the adhesive material. Considering the similar failure pattern, the strength of the timber substrate becomes the governing parameter for adhesives with intermediate and high stiffness. The individual test results are given in Table 2. The characteristic breaking stress $R_{u,5}$ (5%-quantile with 75% confidence) yields for both stiff adhesives to approximately 2,1 MPa. This is more than double the characteristic strength of the silicone adhesive tested within the scope of this study. Ottocoll S660 achieved a $R_{u,5}$ around 0,9 MPa.

Table 2 Shear test results of mid-size specimens, numbers in bold relate to the representative graphs shown in Fig. 11

	A – Ottocoll® S660				B – nolax C44.8505				C – Scotch-Weld™ DP490			
Specimen No.	F_{max} [kN]	Δx [mm]	τ_{max} [N/mm²]	tan γ [-]	F_{max} [kN]	Δx [mm]	τ_{max} [N/mm²]	tan γ [-]	F_{max} [kN]	Δx [mm]	τ_{max} [N/mm²]	tan γ [-]
1	21.8	5.2	0.91	1.73	81.4	1.0	3.39	0.35	74.3	-0.016	3.10	-0.005
2	22.5	5.5	0.94	1.82	89.1	0.7	3.71	0.24	104.0	0.002	4.33	0.001
3	24.1	5.8	1.01	1.93	76.1	0.8	3.17	0.26	73.0	0.015	3.04	0.005
4	24.3	5.8	1.01	1.93	65.2	0.6	2.72	0.20	107.3	0.012	4.47	0.004
5	23.9	5.8	1.00	1.93	92.2	1.3	3.84	0.44	91.2	-0.012	3.80	-0.004
6	–	–	–	–	64.7	0.4	2.70	0.15	74.9	0.001	3.12	0.000
X_{mean}	23.3	5.6	0.97	1.87	78.1	0.8	3.25	0.27	87.4	-0.007	3.64	0.00
σ_X			0.05				0.49				0.65	
$\tau_{\alpha\beta}$	n = 5		2.464		n = 6		2.336		n = 6		2.336	
$R_{u,5}$			0.86				2.12				2.12	

5.3. Comparison of experimental and numerical data

Fig. 13 to Fig. 15 display the stress distribuation along the periphery of the glass pane. The results from the numerical simulation are plotted along the vertical and lower horizontal edge. The presented stress acts in the direction of the edge orientation. The data is compared to the stresses converted from the strain measured at four different positions during the experiments.

The general shape of the stress curve is similar for all examined materials. A significant stress peak in tension develops in the vertical edge within the first 100 mm from the top. The remaining part of the vertical edge is under compression. The highest tensile stress evolves from the model comprising a stiff joint made from Scotch-Weld DP490 (Fig. 15). This adhesive also reveals a significant difference beween the linear and the bilinear approach.

Another maximum of tensile stresses appears as expected in the center of the lower horizontal edge. Both, the silicone and the modified epoxy lead to tensile stresses slightly above 2.0 N/mm^2 at this point. However, the stresses computed in the numerical model drop by approximately 50 % when applying the properties of a stiff epoxy. The measurement result does not change in the same magnitude.

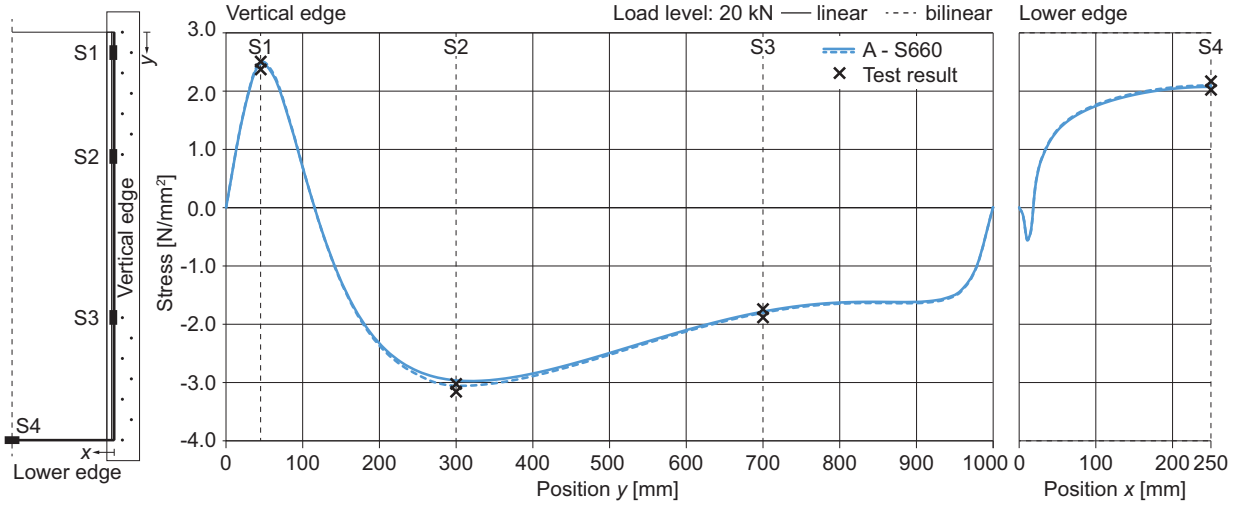

Fig. 13 Calculated stresses along the vertical and the lower horizontal glass edge for A – Ottocoll S660 compared to measured values at the strain gauge positions

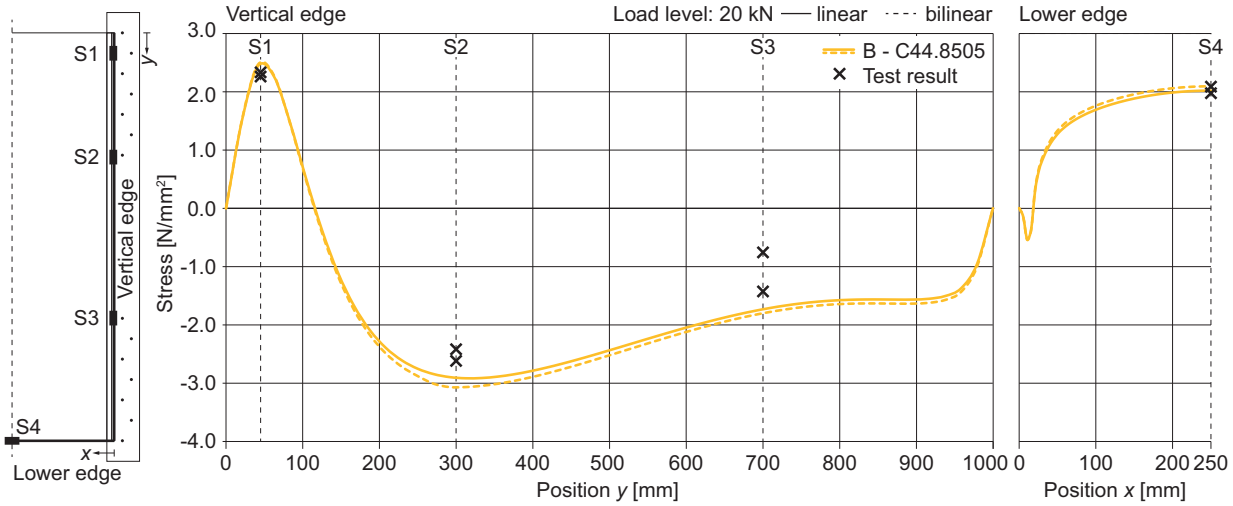

Fig. 14 Calculated stresses along the vertical and the lower horizontal glass edge for B – nolax C44.8505 compared to measured values at the strain gauge positions

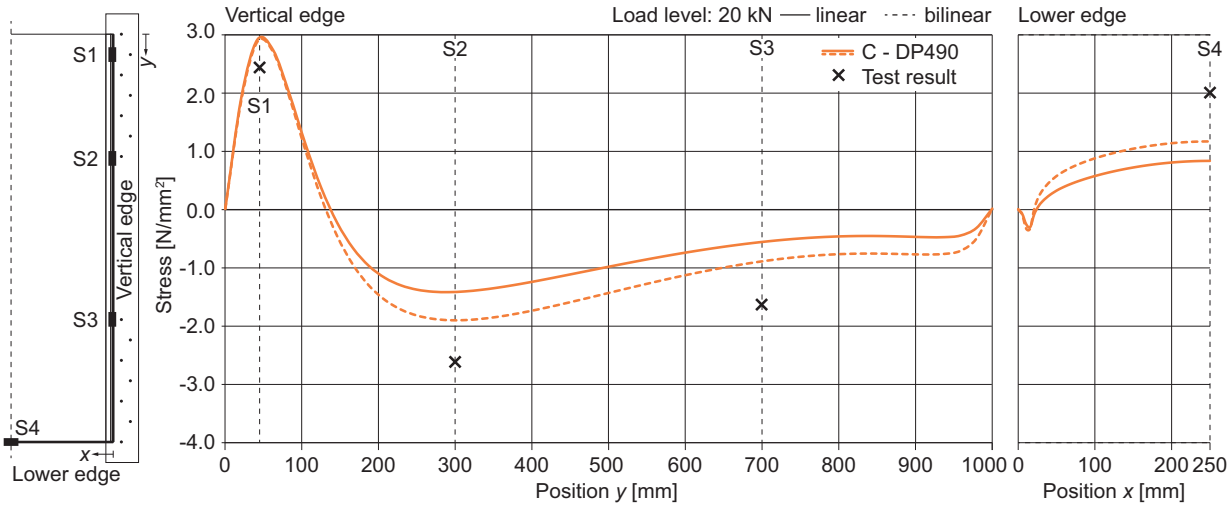

Fig. 15 Calculated stresses along the vertical and the lower horizontal glass edge for C - Scotch-Weld DP490 compared to measured values at the strain gauge positions

The best coincidence between calclulation and experiments is achieved for the flexible silicone adhesive. All strain gauges record strains which match perfectly to the computed stress distribution (Fig. 13). This applies also to nolax C44.8505 (Fig. 14) at the strain gauge positions S1 and S4. But, the numerical simulation leads to higher stresses than recorded by strain gauges at S2 and S3. In contrast, the numerical simulation of the specimen glued with Scotch-Weld DP490 (Fig. 15) underestimates the actual stresses, since the measured values exceed the calculation at three positions. In this case the bilinear model impoves the quality of the results. The computed graph slightly approaches the measurement values. Still, complete aggreement is not reached. Overall, the measured stresses do not vary in the same magnitude than expected from the numerical simulation.

6. Conclusions

The load-bearing behavior of adhesive joints between timber and glass has been assessed under shear loads by means of experimental testing and numerical simulation. Based on the test results it can be concluded that joints with adhesives of high and intermediate stiffness enable an increase of characteristic failure loads and a significant reduction of deformation. With the stiffer joint near-surface rupture of timber fibers becomes the prevailing failure mechanism. The timber strength limits further loading of the adhesive joint.

It could be shown, that – with regard to the stress distribution in the glass pane – linear or bilinear elastic material models provide an adequate approximation of adhesive joints with high flexibility or intermediate stiffness. This is particularly helpful for the estimation of glass stresses in timber-glass composite elements. However, it is not fully achieved to precisely predict the shear deformation of the joint with such a basic numerical simulation. Especially high modulus adhesives require a more sophisticated description of its nonlinear material behavior to impove the aggreement of numerical and experimental results.

Acknowledgements

The research was part of the transnational WoodWisdomNet project “LBTGC - Load Bearing Timber Glass Composites”. The Authors received funding from the German Federal Ministry for Education and Research (BMBF). The adhesives were provided by the respective manufacturers. The authors are also thankful to the Gumpp & Maier GmbH, Binswangen for their help to produce the specimens.

References

Edl, T.: Entwicklung von wandartig verklebten Holz-Glas-Verbundelementen und Beurteilungen des Tragverhaltens als Aussteifungsscheibe. Doctoral thesis, Technische Universität Wien (2008).

Finnforest: Handbuch über Finnisches Sperrholz. Verband der Finnischen Forstindustrie, Lahti (2001).

Hamm J.: Development of Timber-Glass Prefaricated Structural Elements. Innovative Wooden Structures and Bridges. IABSE Conference Report, Vol. 85, pp. 41-46 (2001).

Hochhauser, W., Winter, W., Fadai, A.: Entwicklung von verklebten Holz-Glaskonstruktionen, Bemessung und Anwendung [Development of load bearing timber-glass composites. Design and application]. In: Weller, B., Tasche, S. (eds.), Glasbau 2013, pp. 186-191. Ernst & Sohn, Berlin (2013).

Nicklisch, F., Dorn, M., Weller, B., Serrano, E.: Joint study on material properties of adhesives to be used in load-bearing timber-glass composite elements. engineered transparency | international conference at glasstec | 2014, Düsseldorf, Germany (2014), pp. 271-280.

Niedermaier P.: Holz-Glas-Verbundkonstruktionen. Ein Beitrag zur Aussteifung von filigranen Holztragwerken. Doctoral thesis, Technische Universität München (2005).

uniGlas® GmbH: Handbuch für die Planung und Erstellung von uniGlas® | FACADE Holz-Glas-Verbundelementen. uniGlas® GmbH & Co. KG, Montabaur (2014).

Weller, B., Aßmus, E., Nicklisch F.: Assessment of the Suitability of Adhesives for Load-Bearing Timber-Glass Composite Elements. Proceedings of Glass Performance Days 2013, Tampere, Finland (2013), pp. 54-58.